Journal of the Serbian Chemical Society
JSCS-info@shd.org.rs • www.shd.org.rs/JSCS
J. Serb. Chem. Soc. *90* (7–8) 883–897 (2025)
JSCS–5427
Original scientific paper
Published 18 July, 2025

The role of non-covalent interactions in the solvation dynamics of metronidazole in water: A theoretical study

SUMIT KUMAR[1]*, NAGENDRA KUMAR[1], RAVINDRA KUMAR[1] and KAMAL K. MISHRA[2]

[1]*PG Department of Chemistry, Magadh University, Bodh Gaya 824234, India and* [2]*University of Kentucky, Lexington, Kentucky-40506, USA*

(Received 13 August, revised 1 September 2024, accepted 20 May 2025)

Abstract: Metronidazole, the medicine with the brand name Flagyl, is used to treat the gastrointestinal infection and the activity against anaerobic bacteria like protozoa. The current work describes the interaction of metronidazole drug with water solvent needed for oral ingestion, which is the most common and convenient pathway for the administration of the drug in the body. Computational calculations are performed to optimize the metronidazole drug having solvent (water) at different positions. NBO and AIM calculations employed to determine the strength of intermolecular hydrogen bonding interactions between metronidazole and solvent (water). The second perturbation energy was calculated and the result was a maximum of 67 kJ mol^{-1} for O–H···O hydrogen bonding interaction. The solvation energy of the metronidazole drug, determined using the solvation model based on density (SMD) model, is found to be –69.2 kJ mol^{-1}. The bonding parameters of the solvated drug have been analysed through critical point calculations based on the atom-in-molecule (AIM) theory. Furthermore, an *ab initio* molecular dynamics (AIMD) study reveals that the lowest decomposition energies of metronidazole in the presence of water, considering all pores and different pores, are –927.86 and –699.003 a.u., respectively.

Keywords: drug; flagyl; gastrointestinal infection; SMD; AIM; NBO.

INTRODUCTION

Metronidazole [1-(2-hydroxyethyl)-2-methyl-5-nitroimidazole] is a well-known drug for gastrointestinal infection and popularly used in Flagyl medicine.[1–3] The compound show activity against both gram-negative and gram-positive anaerobic bacteria as well as protozoa. It is previously found effective against protozoan such as giardia lamblia, entamoeba histolytica.[4,5] It has rapid as well as effective abs-

* Corresponding author. E-mail: sumitkrmgr@gmail.com
https://doi.org/10.2298/JSC240813037K

orption due to its smaller molecular structure. It penetrates all tissues such as bones and blood bone barrier.[4–6]

Oral ingestion is the most common and preferred route for drug administration due to its cost-effectiveness, patient compliance, and dosage flexibility.[7] Nearly two-thirds of small-molecule drugs are delivered orally, accounting for about 90 % of the global medicine market, valued at approximately $35 million.[8,9] However, poor solubility remains a major challenge, affecting dissolution rate, efflux susceptibility and first-pass metabolism.

Solvation plays a crucial role in determining a drug's ability to achieve the therapeutic concentrations necessary for effective medicinal application. The pharmacological efficacy of a drug is strongly influenced by its aqueous solubility; therefore, poorly soluble drugs often fail to attain the required plasma concentrations for optimal therapeutic action. Limited water solubility adversely affects the drug's formulation, bioavailability and disaggregation in pharmaceutical preparations. Moreover, the low solubility and poor dissolution rate of sparingly soluble drugs can lead to suboptimal absorption in the gastrointestinal tract, potentially causing adverse effects and compromising oral drug delivery. In this context, the solvation dynamics of metronidazole are investigated to obtain molecular-level insights into its solubility behaviour. These dynamics play a pivotal role in determining its oral bioavailability, dissolution rate, and hydrogen bonding interactions with the aqueous environment – factors that are essential for the effective drug absorption and pharmacological performance. Additionally, a detailed analysis of the non-covalent interactions between metronidazole and water at different solvation sites has been conducted to provide the mechanistic insights into its solvation characteristics.

COMPUTATIONAL DETAILS

Structural conformation

Structural confirmation of metronidazole is performed using Vconf software.[10,11] This software is an important tool for conformational search through the second generation mining minimum algorithm and it utilizes free energy of the molecular system.

Structure optimization

A quantitative study of the interaction between molecules in complexes has been performed. The structural optimization and binding energy calculations along with electrostatic potential have been carried out using Turbomole[12,13] and G09[14] quantum calculation package and graphical user interface TmoleX[15] and Gview.[16] To evaluate the reliability and consistency of the computed structural and energetic parameters, calculations were performed using a range of electronic structure methods, including the hybrid functional B3LYP,[17] the meta-hybrid functional M05-2X[18] known for its improved treatment of noncovalent interactions, the dispersion-corrected B97-D[19] functional, and the correlated wavefunction-based MP2[20,21] method. All computations employed the correlation-consistent triple-ζ quality basis set, cc-pVTZ,[22-24] which offers a balanced description of valence electron correlation. This multi-level approach ensures a robust comparison, with a higher level than the density functional and post-Hartree–

–Fock frameworks, particularly in capturing subtle intermolecular interactions. Harmonic vibrational frequency analyses were carried out for the conformers of metronidazole at several theoretical levels to ensure that the optimized structures represented true local minima. The interaction energies of different conformers were refined by incorporating corrections for both basis set superposition error (*BSSE*) and zero-point vibrational energy (*ZPE*). *BSSE* was accounted for using the counterpoise technique proposed by Boys and Bernardi.[25]

Natural bond orbital (NBO), non-covalent interactions (NCI), atom in molecule (AIM) and eenergy decomposition analysis (EDA) study

The NBO analysis provides insights into bonding, electron density, and charge transfer, while NCI analysis quantifies non-covalent interactions like hydrogen bonding and van der Waals forces.[26-28] AIM analysis offers a topological view of electron density, and EDA quantifies intermolecular interactions. Geometry optimizations at the M05-2X/cc-pVTZ[18,22-24] level were used for NBO,[29] NCI,[28] AIM[30] and EDA analyses.[31] NCI calculations were performed using NCIPLOT,[28] AIM using Multiwfn,[32-34] and NBO using G09 with NBO7.[27] The intermolecular interaction energies in dimer and trimer systems were analysed via EDA using the localized molecular orbital (LMO) approach in the GAMESS (U.S.A.) program.[35]

Solvation study

A solvation study involves analysing the interactions and effects of a solvent on a solute. One effective approach to incorporating solvent effects is through implicit solvation models such as the SMD model.[36,37] Developed by the Cramer and Truhlar research groups, the SMD solvation model has been applied to investigate the solvent influence on metronidazole. This advanced continuum solvation method is based on the quantum mechanical charge density of the solute, treating the solvent as a continuous medium. The term "SMD" signifies the direct use of full electron density ("D" for density) without the need to define partial atomic charges. Rather than explicitly modelling solvent molecules, this approach represents the solvent as a dielectric medium with surface tension at the solute–solvent interface, providing a more efficient and accurate depiction of solvation effects.[37] The model uses the full solute electron density without explicit charges on solute whereas uses the surface tension over the solute–solvent boundary.

The implicit solvation model is applied for the study of solvation of Metronidazole using at PBE0-D3/def2-TZVP[38-40] "tightopt" level. The solvated free energy change (ΔG_{solv}) can be calculated using the equation: $\Delta G_{solv} = E_{solv} + \Delta G_{el} + (\Delta G_{cav} + \Delta G_{disp})$. It includes liquid phase expectation value, electron-polarization and non-electrostatic contribution. The non-electrostatic contribution (ΔG_{net}) of the solvated system includes cavitation energy (ΔG_{cav}) and the dispersion energy (ΔG_{disp}) during solvation of the solute.

Ab initio *molecular dynamics assay*

Ab initio molecular dynamics (AIMD) study has already shown some significant benefits over traditional molecular dynamics.[41,42] AIMD is on-the-fly method to obtained electronic structure related information from the recent trajectory. AIMD study is performed for Metronidazole with water using ORCA 5.0.3 software[43] at a timestep of 1.0 fs. The temperature was kept constant at 350 K whereas Timecon of 10.0 fs is used. The study was performed at PBE0--D3/def2-SVP level of theory using Orca 5.0.3.43 The interesting fact was that the variation in energy scales between the SMD implicit the solvation model and the AIMD arises from their distinct methodologies. The SMD uses a static, continuum approach that approximates solvation effects without explicit solvent molecules or thermal fluctuations, yielding single-point

energies. In contrast, AIMD includes the explicit solvent interactions and thermal motion, providing time-averaged energies that account for entropic and dynamic effects.

RESULTS AND DISCUSSION

Geometry of metronidazole and its solvated structure

The lowest-energy conformer of Metronidazole, identified using Vconf and binding energy calculations (Fig. 1a), is reported in the Supplementary material to this paper. It comprises 21 atoms: 3 nitrogen, 3 oxygen, 6 carbon and 9 hydrogen. The solvated metronidazole has water at four positions, which are pore1, pore2, pore3 and pore4. These optimized geometries are abbreviated considering the position of water, which are Met-wtr.P1, Met-wtr.P2, Met-wtr.P3 and Met-wtr.P4, respectively (see Fig. 1) at B3LYP/cc-pVTZ level of theory. Optimized coordinates of metronidazole and its complexes (Met-wtr.P1–P4, All) at the M05-2X/cc--pVTZ level are provided in Tables S-XI–S-XVI of the Supplementary material. The corresponding binding energies with BSSE correction (ΔE_e) are calculated –53.09, –39.83, –40.12 and –30.38 kJ mol^{-1}, respectively, whereas the binding energies with both BSSE and zero-point energy correction (ΔE_o) are calculated –43.76, –31.25, –31.97, and –23.56 kJ mol^{-1}, respectively (see Table I). Eventually the completely solvated metronidazole has all pores filled with water molecules, which is abbreviated as Met-wtr.All. Interestingly, the ΔE_e and ΔE_o values for completely solvated metronidazole at all pores is calculated –164.35 and –131.84 kJ mol^{-1}, respectively. The full vibrational frequency analyses at DFT-in the Supporting material to this paper-optimized geometries confirmed all stationary points as true local minima, with no imaginary frequencies observed.

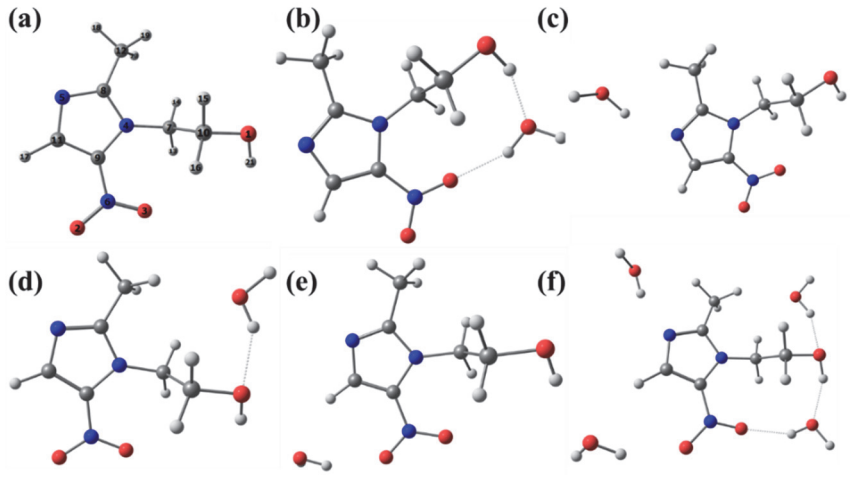

Fig. 1. Optimized structures of: a) Metronidazole, b) Met-wtr.P1, c) Met-wtr.P2, d) Met-wtr.P3, e) Met-wtr.P4 and f) Met-wtr.All at M05-2X/cc-pVTZ level of theory.

TABLE I. Binding energies (in kJ mol^{-1}) for complexes of metronidazole with water solvent molecules

Geometry	B3LYP/cc-pVTZ		M05-2X/cc-pVTZ		B97D/cc-pVTZ		MP2/cc-pVTZ	
	ΔE_e	ΔE_o	ΔE_e	ΔE_o	ΔE_e	ΔE_o	ΔE_e	ΔE_o
Met-wtr.P1	–53.09	–43.76	–134.31	–125.35	–55.98	–47.40	–41.00	–31.97
Met-wtr.P2	–39.83	–31.25	–117.53	–108.53	–40.00	–31.97	–28.70	–20.21
Met-wtr.P3	–40.12	–31.97	–124.06	–115.10	–46.69	–38.28	–30.79	–22.38
Met-wtr.P4	–30.38	–23.56	–107.74	–101.00	–30.00	–23.97	–22.68	–16.15
Met-wtr.All	–164.35	–131.84	–457.39	–424.59	–175.94	–144.01	–84.56	–52.22

In Met-wtr.P1, O1-H21 and O22-H24 bond lengths are 0.96748 and 0.96274 Å, respectively. The corresponding lengths in bare metronidazole and water molecule are 0.95884 and 0.95742 Å, respectively. The increase of bond lengths is attributed to O22···O1–H21 and O3···O22–H24 hydrogen bonding interactions. O22–H24 and C12–H18 bond lengths are 0.96876 and 1.08469 Å, respectively in Met-wtr.P2. The hydrogen bonding interactions such as N5···O22–H24 and O22···C12–H18 are responsible for the increase of bond lengths in Met-wtr.P2. Furthermore O1···O22–H24 and O22···C11–H17 as well as O2···O22–H23 hydrogen bonding interactions are present in Met-wtr.P3 and Met-wtr.P4, respectively.

Charge density analysis of the solvated metronidazole

Mulliken population analysis (MPA) charges of metronidazole–water complexes at four positions (Met-wtr.P1, Met-wtr.P2, Met-wtr.P3, Met-wtr.P4) were calculated at the M05-2X/cc-pVTZ level and are presented in Fig. S-1 of the Supplementary material, with the corresponding data provided in Table S-V of the Supplementary material. The study reveals a decrease in the MPA charge of oxygen O22 from–0.4783 e in bare water to -0.5027, –0.5073, –0.4858 and –0.4877 e in Met-wtr.P1, P2, P3 and P4, respectively, due to hydrogen bonding. MPA charges of O1 and O3 in Met-wtr.P1 increased to –0.3896 and –0.3833 e from –0.3648 and –0.3249 e in bare metronidazole, influenced by O1–H21···O22 and O22–H24···O3 hydrogen bonding. Similarly, the charge of N5 in Met-wtr.P2 rose to –0.3140 from –0.2568 e due to N5···O22–H24 bonding. MPA charges of O1 in Met-wtr.P3 and O2 in Met-wtr.P4 were –0.32804 and –0.27956 e, respectively, reflecting changes due to hydrogen bonding interactions (O1···O22–H24 in Met--wtr.P3 and O2···O22–H23 in Met-wtr.P4).

HOMO–LUMO energy variation of the metronidazole

HOMO and LUMO energies provide crucial chemical information. E_{HOMO} relates to electron donation ability, while E_{LUMO} is related to the electron acceptance. Higher E_{HOMO} increases electron donation tendency, requiring less energy for electrons to jump to unoccupied states. Lower E_{LUMO} enhances electron acceptance. For metronidazole, E_{HOMO} and E_{LUMO} are –7.075 and –2.441 eV,

respectively. On water solvation, E_{LUMO} values for Met-wtr.P1, Met-wtr.P2, Met--wtr.P3, Met-wtr.P4 and Met-wtr.All are –2.716, –2.664, –2.351, –2.699 and –3.045 eV, showing decreased electron acceptance. E_{HOMO} values for these are –7.023, –7.347, –6.939, –7.173 and –7.293 eV, indicating a higher electron donation tendency. Met-wtr.All has a band gap of 4.249 eV, with ionization energy, electron affinity, chemical hardness, electronic chemical potential and electrophilicity index calculated as 7.293, 3.045, 2.124, –5.169 and 12.579 eV, respectively. Various other molecular parameters in order to understand the characteristics features of metronidazole. Various other molecular parameters in order to understand the characteristics features of metronidazole along with water are shown in Table S-I of the Supplementary material.

Solvation of Metronidazole

Solvation model mimics the environment of multiple solvation shells without placing it close to the drug. Metronidazole drug is soluble in water and all the atoms of metronidazole are close to the boundary along with the solvent. Table S-III of the Supplementary material also shows the solvation data with other solvents. The result shows that surface charge (e) indicates the electrostatic contribution to solvation free energy from interactions between the solute's charge distribution and the solvent environment. Water exhibits the highest surface charge (–28.207 e), reflecting its high polarity and strong electrostatic interactions with the solute. Nonpolar solvents like tetrahydrofuran (THF) and chloroform have smaller surface charge values (–14.531 e and –16.932 e, respectively), consistent with weaker electrostatic interactions. Charge correction is a correction term for inaccuracies in the computed electrostatic interactions. The values are very small (0.02–0.03), indicating minimal correction is needed, which suggests the computational model accurately represents the solvent environment. The free energy (cavitation + dispersion) represents the combined free-energy contributions from cavity formation (to accommodate the solute) and van der Waals dispersion interactions between solute and solvent. Water shows the largest positive value (18.853 kJ mol^{-1}), reflecting a significant cost of cavity formation and weak dispersion interactions. Solvents like pyridine and THF have more negative values (–16.342 and –15.790 kJ mol^{-1}), indicating more favourable van der Waals dispersion contributions.

The single point energies of metronidazole and Metronidazole–water system are –623.4575 and –623.4774 a.u., respectively. Therefore, the solvated system of Metronidazole with water has stabilization energy of –0.0199 a.u., *i.e.*, –52.245 kJ mol^{-1}.

Using SMD solvation model, CPCM the dielectric energy is calculated –95.980 kJ mol^{-1} and the energy of cavity dispersion solvated system (SMD CDS (Gcds)) in the water solvent is calculated –0.0264 a.u., *i.e.*, –69.203 kJ mol^{-1}.

Non-covalent interactions (NCI) of Metronidazole

NCI analysis provide electron density (s) and reduced density gradient (ρ) for solvated metronidazole in different pores (Fig. S-2 of the Supplementary material). The isosurface extraction of reduced density gradient is depicted in Fig. S-3 of the Supplementary material. Color schemes indicate interaction types: blue for strong attractive, green for weak non-covalent (van der Waals), and red for repulsive forces.[28,44] Spikes in Fig. S-2 indicate interactions, with those between –0.02 and 0.02 representing hydrogen bonding. Greenish–blue overlaps in Fig. 2 illustrate intermolecular hydrogen bonding and some intramolecular interactions within Metronidazole in vicinity of four water molecules only.

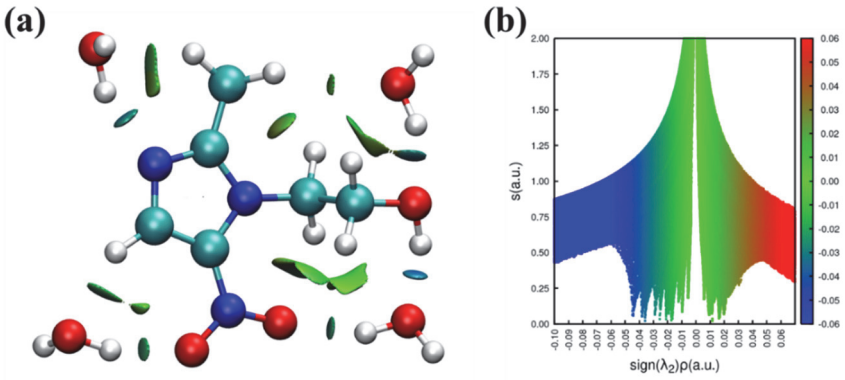

Fig. 2. Isosurface extractions (a) of its RDG plots (b) of NCI analysis of Met-wtr.All.

Energy decomposition analysis (EDA) of Metronidazole with water molecules

The EDA study provides the information regarding the various components of interaction energy for the solvated complexes of metronidazole depending upon the various positions of the water. The total interaction (ΔE_{tot}) is decomposed into exchange energy (ΔE_{ele}), repulsion energy (ΔE_{rep}), polarization energy (ΔE_{pol}) and dispersion energy (ΔE_{disp}). These values are depicted in Table S-II of the Supplementary material. The result assists that the electrostatic component is –70.29 kJ mol^{-1} for Met-wtr.P1, which are –47.95, –46.69 and –30.96 kJ mol^{-1} for Met--wtr.P2, Met-wtr.P3 and Met-wtr.P4, respectively. The dispersion components are calculated –40.29, –27.87, –35.86 and –23.14 kJ mol^{-1}, respectively. Interestingly, the electrostatic component is found nearly double of the dispersion component for Met-wtr.P1 and Met-wtr.P2 whereas the dispersion component is nearly 3/4th of electrostatic component for Met-wtr.P3 and Met-wtr.P4. The high electrostatic component is attributed to the strong hydrogen bonding interaction such as H–O···H, O–H···N. The four hydrogen bonding interactions in Met-wtr.All attributed the increase of electrostatic component in comparison to dispersion component.

Natural bond orbital (NBO) study of Metronidazole

NBO analysis was performed for all four pore positions of water near Metronidazole, as well as for metronidazole occupying each pore with surrounding water molecules.[45] Second order perturbation energy or donor-acceptor interaction energy, $E_{i\rightarrow j}^{(2)}$, the most important parameter, has been evaluated for all interactions between NBO donor (i) and acceptor (j).[26,46]

The NBO study is performed for metronidazole with water solvent at all four pores or position. At pore1, the water molecule is situated in the pore between nitro- and hydroxyl-groups. In pore2, the water molecule is placed at the pore close to N5 and methyl group (close to H18) of metronidazole while the water molecule is placed closed to methyl and hydroxyl groups (close to O1) of Metronidazole in pore3. In pore4, the water takes the place close to nitro group and H17. In case of Met-wtr.All, all the pores are occupied by water molecules.

Fig. 1 shows the structures of Metronidazole having water at different pores and all pores. Several other interactions are calculated between metronidazole and water molecules (see Table S-IV of the Supplementary material). Fig. S-4 of the Supplementary material shows the NBO overlap for the important non-covalent interactions for Met-wtr.P1, Met-wtr.P2, Met-wtr.P3 and Met-wtr.P4. In Met--wtr.P1, the major interaction of the bonding orbitals LP(2)O22 and LP(1)O3 has been found with BD*(1)O1-H21 and BD*(1)O22-H24 due to H–O···H conventional hydrogen bonding. The $E_{i\rightarrow j}^{(2)}$ value for the corresponding interaction has been calculated 64.48 and 16.32 kJ mol^{-1}, respectively. Similarly, Met-wtr.P2 complexes show the strong hydrogen bonding interaction between metronidazole and water. The interaction has been reported between bonding orbitals of LP(1)N5 and LP(2)O22 with antibonding orbitals BD*(1)O22-H24 and BD*(1)C12-H18 whereas the $E_{i\rightarrow j}^{(2)}$ values are 46.65 and 11.00 kJ mol^{-1}, respectively. Further solvated metronidazole having water in pore3 interacts through its hydroxyl and methyl groups therefore the O1···O22–H24 hydrogen bonding interaction stabilizes the complexes. Both the lone pairs of oxygen interaction with hydrogen bond acceptor O22–H24. Met-wtr.P4 having water in pore 4 of metronidazole interacts through double hydrogen bonding interaction, where the electron delocalization of electron transfer of lone pairs of O22 and O2 to acceptor antibonding orbital BD*(1)C11-H17 and BD*(1)O22-H23, respectively. The second order perturbation energy is calculated 15.61 and 13.51 kJ mol^{-1}, respectively.

It is interesting that in the case of the Metronidazole–water complex in the solvated state, Met-wtr.All, multiple hydrogen bonding interactions form to stabilize the complex utilizing the water molecules sitting at four pores or positions close to metronidazole. The important interactions are highlighted in Fig. 3. Interestingly O22···O1–H21 and O3···O22–H24, N5···O25–H27 and O25···C12–H18, O1···O31–H33 and O28···C11–H17, and O2···O28–H29 hydrogen bonding interactions take place with water sitting at the pore1, pore2, pore3 and pore4, respectively. The

related data has been kept in Table S-IV. The interaction between LP(2)O22 (lone pair on oxygen of metronidazole) and BD(1)O1-H21* (antibonding orbital of a water O–H bond) exhibits the highest stabilization energy of 69.91 kJ mol^{-1}. This indicates a strong hydrogen bond or significant charge transfer from the lone pair of oxygen on metronidazole to the O–H antibonding orbital of water.

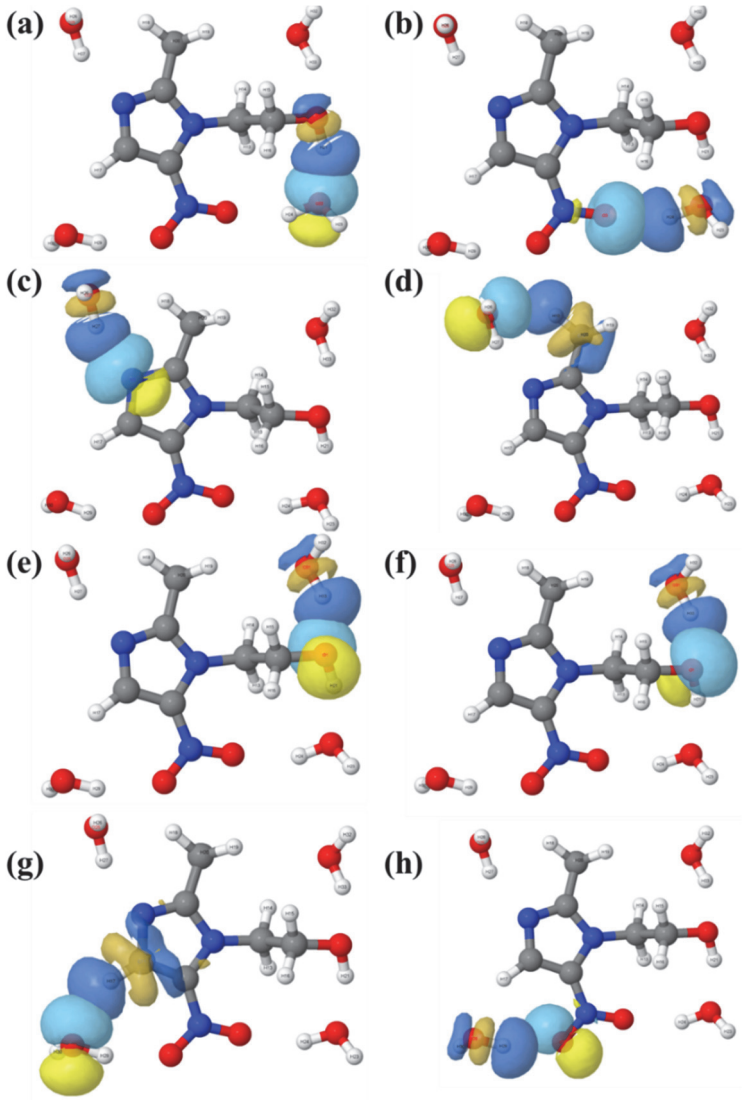

Fig. 3. NBO interaction of: a) LP(2)O22→BD*(1)O1-H21, b) LP(1)O3→BD*(1)O22-H24, c) LP(1)N5→BD*(1)O25-H27, d) LP(2)O25→BD*(1)C12-H18, e) LP(2)O1→BD*(1)O31-H33, f) LP(1)O1→BD*(1)O31-H33, g) LP(2)O28→BD*(1)C11-H17 and h) LP(2)O2→BD*(1)O28-H29 for Met-wtr.All.

The lone pair on the nitrogen atom (N5) interacts with the antibonding orbital of another O–H bond in water, forming another relatively strong hydrogen bond. A lone pair on oxygen (likely a ring oxygen in metronidazole) participates in a hydrogen bond with a water molecule. Interactions involving LP(2)O28, LP(1)O3, LP(2)O2 and LP(2)O25 with various antibonding O–H and C–H orbitals of water or Metronidazole result in lower stabilization energies (ranging from 9.92 to 18.03 kJ mol^{-1}). These are weaker hydrogen bonds or dipolar interactions.

The interactions suggest a robust hydrogen bonding network between Metronidazole and water molecules. This network stabilizes the solvation environment around Metronidazole and facilitates its bioactivity in aqueous systems. The oxygen atoms (O22, O1, O28, O3, O2, O25) are the dominant donors, emphasizing their nucleophilicity and involvement in hydrogen bonding. The nitrogen lone pair (LP(1)N5) also plays a significant role, suggesting its participation in hydrogen bonding or electronic delocalization.

Atom-in-molecule (AIM) analysis for Metronidazole

The AIM study is eligible to provide essential information regarding atom––atom interactions in through either covalent or non-covalent interaction molecular cluster, molecular crystal, *etc*.[30] This study provides important tools to measure the electron density, $\rho(r)$ and Laplacian of electron density, $\nabla^2\rho_{bcp}(r)$ at a bond critical point (BCP).[47] The yellow lines connecting two closely lying molecules consists small red spheres indicating BCP. AIM calculation measures various topological parameters at these BCPs. The position of the BCP changes depending upon the electronegatively of the connected atoms. The AIM study for Metronidazole with water, *i.e*., Met-wtr.P1, Met-wtr.P2, Met-wtr.P3, Met-wtr.P4 and Met--wtr, which are all reported in Fig. S-1 of the Supplementary material. The corresponding data has been shown in Tables SVI–SX of the Supplementary material.

Met-wtr.P1 is stabilised by hydrogen bonding interaction between Metronidazole and water. Hydrogen bonding between H21···O22 and O3···H24 mainly stabilize the molecule. The corresponding BCPs between these atoms has $\rho(r)$ of –0.00364 and 0.003184 a.u. whereas $\nabla^2\rho_{bcp}(r)$ values of 0.111881 and 0.093755 a.u., respectively. In case of Met-wtr.P2, the water molecule is in the pores close to methyl group of metronidazole and interacts through intramolecular O22···H18 and intermolecular H16···O3 hydrogen bonding interactions. The electron density, $\rho(r)$ for these BCPs are 0.001712 and 0.002167 a.u., respectively whereas $\nabla^2\rho_{bcp}(r)$ for these points are reported 0.035909 and 0.048868 a.u., respectively. In case of metronidazole with water molecule in the pore3, Met-wtr.P3, the water molecule is close to methyl and hydroxy groups therefore linked through O22···H19, O22···H14, O3···H16 and O1···H24 hydrogen bonding interactions. The corresponding $\nabla^2\rho_{bcp}(r)$ values are reported 0.027317, 0.034301, 0.038455 and 0.10487 a.u., respectively. Met-wtr.P4 complex between metronidazole and water stabilize

through intermolecular H16···O3, H17···O22, H23···O2 hydrogen bonding interactions while the intramolecular H13···O3 hydrogen bonding interaction also helps the stability of molecule.

Furthermore, metronidazole occupied with all four pores by water molecules interact with multiple hydrogen bonding interaction as understood through AIM study. The complexes stabilize through H13···O3, H16···O3, H24···O3, H17···O28, H29···O2, H18···O25, H14···O31 and H19···O31 hydrogen bonding interactions.

Ab initio *molecular dynamics assay of metronidazole*

AIMD study[41,42] has been performed for metronidazole with water and reported in Fig. 4. The molecular dynamics study was used to understand the velocity of boundary atoms around the metronidazole along with solvated water. Fig. 4 represents the total energy of solvated metronidazole with water versus time (in fs). The total energy is the cumulative of total potential and kinetic energies.

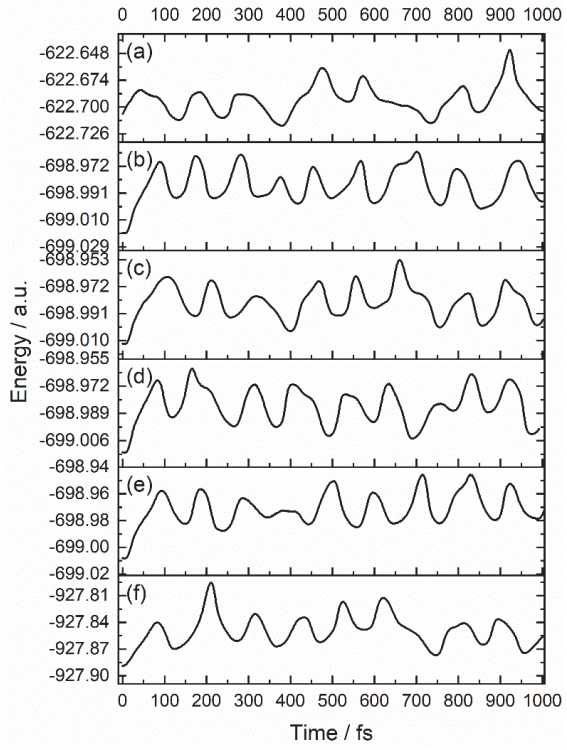

Fig. 4. Simulation of solvated metronidazole with water: a) Metronidazole, b) Met-wtr.P1, c) Met-wtr.P2, d) Met-wtr.P3, e) Met-wtr.P4, f) Met-wtr.All.

The study reveals that the lowest decomposition energy for Metronidazole with water at all pores (Met-wtr.All) is -927.86 a.u. (see Fig. 4f), representing the

most stabilized configuration. This value is significantly lower than the lowest decomposition energies for Metronidazole with water at individual pores (Met--wtr.P1 to Met-wtr.P4), which are approximately –699.003 a.u. The results indicate that the presence of water molecules at all interaction sites around Metronidazole contributes to enhanced stabilisation, as reflected in the much lower decomposition energy. This finding highlights the importance of a fully solvated environment in achieving maximum stability for the system. Furthermore, the lowest decomposition energy for Met-wtr. All was observed between 700–800 fs, consistent with the system reaching its most stable state during this timeframe. The calculated decomposition energies from AIMD simulations align well with the total energy values obtained from quantum chemical calculations, reinforcing the reliability of the results. This correlation underscores the critical role of complete solvation in stabilizing metronidazole, providing valuable insights into its behavior in aqueous environments.

The gradual stabilisation of the Met–wtr system reflects the cumulative impact of hydrogen bonding and electrostatic interactions as water molecules cluster around metronidazole. This supports the notion that metronidazole forms strong solute–solvent interactions, enhancing its solubility and bioavailability in aqueous environments. The oscillatory nature of the energy profiles indicates that solvation dynamics are not static but evolve over time. The system achieves local energy minima due to non-covalent interactions, but the thermal motion causes periodic fluctuations. The trend observed in the data is consistent with solvation theory, where the introduction of polar solvents like water leads to increasing stabilization due to non-covalent interaction networks.

CONCLUSION

Metronidazole is an important drug against gastrointestinal infection, Gram--negative and Gram-positive anaerobic bacteria as well as protozoa. The structures of metronidazole and its solvated structures are studied. The solvation of Metronidazole with solvent (water) is investigated based on SMD model and the free energy is calculated –0.0264 a.u., *i.e.*, –69.20 kJ mol^{-1}. AIMD studies has been performed in order to study the velocity of boundary atoms around Metronidazole and the lowest decomposition energies are calculated 699.003 and –927.86 a.u. for metronidazole with water at pore1–pore4 and all pores, respectively. The solvated structure of metronidazole is found stabilized mainly through multiple O–H···O hydrogen bonding interactions. The EDA calculations describes that hydrogen bonding, van der Waals and steric repulsion play a main role in the stability of the solvated metronidazole. The NBO study explains that $E^{(2)}_{i\rightarrow j}$ value for the interaction has been calculated 64.48 and 16.32 kJ mol^{-1}, respectively. The results obtained from the solvation dynamics may significantly influence the Metronidazole's oral uptake, the rate of dissolution, and the intermolecular interactions with

the surrounding water molecules key aspects that govern its absorption efficiency and the therapeutic effectiveness.

SUPPLEMENTARY MATERIAL

Additional data and information are available electronically at the pages of journal website: https://www.shd-pub.org.rs/index.php/JSCS/article/view/13011, or from the corresponding author on request.

Acknowledgement. SK expresses gratitude to Magadh University, Bodh Gaya, Bihar, India, for the laboratory facilities and acknowledges the Science and Engineering Research Board (SERB), Department of Science & Technology (DST), India (Grant No. SRG/2019/ /002284), for financial assistance.

ИЗВОД

УЛОГА НЕКОВАЛЕНТНИХ ИНТЕРАКЦИЈА У ДИНАМИЦИ РАСТВОРА МЕТРОНИДАЗОЛА У ВОДИ: ТЕОРИЈСКА СТУДИЈА

SUMIT KUMAR[1], NAGENDRA KUMAR[1], RAVINDRA KUMAR[1] and KAMAL K. MISHRA[2]

[1]PG Department of Chemistry, Magadh University, Bodh Gaya 824234, India и [2]University of Kentucky, Lexington, Kentucky-40506, USA

Метронидазол, под трговачким именом Flagyl, користи се за лечење гастроинтестиналних инфекција и има активност против анаеробних бактерија и протозоа. Овај рад описује интеракцију метронидазола са водом као растварачем, који је неопходан за оралну примену, што је најчешћи и најпогоднији начин за примену лекова у организму. Рачунарски прорачуни су изведени ради оптимизације структуре метронидазола са растварачем (водом) постављеним на различите позиције. NBO (прорачуни засновани на везивним природним орбиталама) и AIM (теорија атома у молекулима) прорачуни су примењени за одређивање јачине интермолекулских водоничних веза између метронидазола и растварача (воде). Пертурбациона енергија другог реда показује максималних 67 kJ mol^{-1} за O–H···O водоничну везу. Енергија солватације метронидазола, одређена коришћењем SMD модела (модел солватације заснован на густини), износи –69,2 kJ mol^{-1}. Параметри везивања солватисаног лека су анализирани помоћу прорачуна критичних тачака, а на основу AIM теорије. *Ab initio* молекулска динамика (AIMD) је показала да су најниже енергије декомпозиције метронидазола у присуству воде, узимајући у обзир све поре и различите поре, редом –927,86 и –699,003 a.u.

(Примљено 13. августа, ревидирано 1. септембра 2024, прихваћено 20. маја 2025)

REFERENCES

1. S. Löfmark, C. Edlund, C. E. Nord, *Clin. Infect. Dis.* **50** (2010) S16 (http://dx.doi.org/10.1086/647939)
2. S. Arora, J. Clarke, E. Tsakalozou, P. Ghosh, K. Alam, J. E. Grice, M. S. Roberts, M. Jamei, S. Polak, *Mol. Pharm.* **19** (2022) 3139 (http://dx.doi.org/10.1021/acs.molpharmaceut.2c00229)
3. C. Gao, X. Wang, B. Yang, W. Yuan, W. Huang, G. Wu, J. Ma, *ACS Nano* **17** (2023) 7335 (http://dx.doi.org/10.1021/acsnano.2c11305)
4. D. Pal, S. Banerjee, J. Cui, A. Schwartz, S. K. Ghosh, J. Samuelson, *Antimicrob. Agents Chemother.* **53** (2009) 458 (http://dx.doi.org/10.1128/aac.00909-08)

5. J. Samuelson, *Antimicrob. Agents Chemother.* **43** (1999) 1533 (http://dx.doi.org/10.1128/aac.43.7.1533)
6. R. Nau, F. Sörgel, H. Eiffert, *Clin. Microbiol. Rev.* **23** (2010) 858 (http://dx.doi.org/10.1128/cmr.00007-10)
7. S. V. Sastry, J. R. Nyshadham, J. A. Fix, *Pharmaceut. Sci. Technol. Today* **3** (2000) 138 (http://dx.doi.org/10.1016/S1461-5347(00)00247-9)
8. B. Agoram, W. S. Woltosz, M. B. Bolger, *Adv. Drug Delivery Rev.* **50** (2001) S41 (http://dx.doi.org/10.1016/S0169-409X(01)00179-X)
9. M. Jamei, D. Turner, J. Yang, S. Neuhoff, S. Polak, A. Rostami-Hodjegan, G. Tucker, *AAPS J.* **11** (2009) 225 (http://dx.doi.org/10.1208/s12248-009-9099-y)
10. C.-E. Chang, M. K. Gilson, *J. Comput. Chem.* **24** (2003) 1987 (http://dx.doi.org/10.1002/jcc.10325)
11. S. L. Mayo, B. D. Olafson, W. A. Goddard, *J. Phys. Chem.* **94** (1990) 8897 (http://dx.doi.org/10.1021/j100389a010)
12. Y. J. Franzke, C. Holzer, J. H. Andersen, T. Begušić, F. Bruder, S. Coriani, F. Della Sala, E. Fabiano, D. A. Fedotov, S. Fürst, *J. Chem. Theory Comput.* **19** (2023) 6859 (http://dx.doi.org/10.1021/acs.jctc.3c00347)
13. S. G. Balasubramani, G. P. Chen, S. Coriani, M. Diedenhofen, M. S. Frank, Y. J. Franzke, F. Furche, R. Grotjahn, M. E. Harding, C. Hättig, *J. Chem. Phys.* **152** (2020) 184107 (http://dx.doi.org/10.1063/5.0004635)
14. *Gaussian 09, Revision A.02,* Gaussian, Inc., Wallingford, CT, 2016
15. C. Steffen, K. Thomas, U. Huniar, A. Hellweg, O. Rubner, A. Schroer, *J. Comput. Chem.* **31** (2010) 2967 (http://dx.doi.org/10.1002/jcc.21576)
16. *GaussView*, Semichem Inc., Shawnee Mission, KS, 2016.
17. P. J. Stephens, F. J. Devlin, C. F. Chabalowski, M. J. Frisch, *J. Phys. Chem.* **98** (1994) 11623 (https://doi.org/10.1021/j100096a001)
18. Y. Zhao, N. E. Schultz, D. G. Truhlar, *J. Chem. Theory Comput.* **2** (2006) 364 (http://dx.doi.org/10.1021/ct0502763)
19. S. Grimme, *J. Comput. Chem.* **27** (2006) 1787 (https:/doi.org/10.1002/jcc.20495)
20. M. J. Frisch, M. Head-Gordon, J. A. Pople, *Chem. Phys. Lett.* **166** (1990) 281 (https:/doi.org/10.1016/0009-2614(90)80030-H)
21. M. J. Frisch, M. Head-Gordon, J. A. Pople, *Chem. Phys. Lett.* **166** (1990) 275 (https:/doi.org/10.1016/0009-2614(90)80029-D)
22. D. E. Woon, T. H. Dunning, Jr., *J. Chem. Phys.* **98** (1993) 1358 (http://dx.doi.org/10.1063/1.464303)
23. R. A. Kendall, T. H. Dunning, Jr., R. J. Harrison, *J. Chem. Phys.* **96** (1992) 6796 (http://dx.doi.org/10.1063/1.462569)
24. T. H. Dunning, Jr., *J. Chem. Phys.* **90** (1989) 1007 (http://dx.doi.org/10.1063/1.456153)
25. S. F. Boys, F. and Bernardi, *Mol. Phys.* **19** (1970) 553 (http://dx.doi.org/10.1080/00268977000101561)
26. F. Weinhold, *J. Comput. Chem.* **33** (2012) 2363 (http://dx.doi.org/10.1002/jcc.23060)
27. E. D. Glendening, C. R. Landis, F. Weinhold, *J. Comput. Chem.* **40** (2019) 2234 (http://dx.doi.org/10.1002/jcc.25873)
28. R. A. Boto, F. Peccati, R. Laplaza, C. Quan, A. Carbone, J. P. Piquemal, Y. Maday, A. J. Contreras-Garci, *J. Chem. Theory Comput.* **16** (2020) 4150 (http://dx.doi.org/10.1021/acs.jctc.0c00063)
29. F. Weinhold, C. Landis, E. Glendening, *Int. Rev. Phys. Chem.* **35** (2016) 399 (https://doi.org/10.1080/0144235X.2016.1192262)

30. P. Kolandaivel, V. Nirmala, *J. Mol. Struct.* **694** (2004) 33 (http://dx.doi.org/10.1016/j.molstruc.2004.01.030)
31. P. Su, H. Li, *J. Chem. Phys.* **131** (2009) 014102 (http://dx.doi.org/10.1063/1.3159673)
32. T. Lu, *J. Chem. Phys.* **161** (2024) (http://dx.doi.org/10.1063/5.0216272)
33. T. Lu, Q. Chen, in *Conceptual Density Functional Theory: Towards a New Chemical Reactivity Theory,* Vol. 2, S. Liu, Ed., Wiley-VCH GmbH, Weinheim, 2022, p. 631
34. T. Lu, F. Chen, *J. Comput. Chem.* **33** (2012) 580 (http://dx.doi.org/10.1002/jcc.22885)
35. M. W. Schmidt, K. K. Baldridge, J. A. Boatz, S. T. Elbert, M. S. Gordon, J. H. Jensen, S. Koseki, N. Matsunaga, K. A. Nguyen, S. Su, T. L. Windus, M. Dupuis, J. A. Montgomery Jr, *J. Comput. Chem.* **14** (1993) 1347 (https:/doi.org/10.1002/jcc.540141112)
36. V. Barone, M. Cossi, *J. Phys. Chem., A* **102** (1998) 1995 (http://dx.doi.org/10.1021/jp9716997)
37. A. V. Marenich, C. J. Cramer, D. G. Truhlar, *J. Phys. Chem., B* **113** (2009) 6378 (http://dx.doi.org/10.1021/jp810292n)
38. F. Weigend, *Phys. Chem. Chem. Phys.* **8** (2006) 1057 (http://dx.doi.org/10.1039/B515623H)
39. S. Grimme, S. Ehrlich, L. Goerigk, *J. Comput. Chem.* **32** (2011) 1456 (https:/doi.org/10.1002/jcc.21759)
40. C. Adamo, V. Barone, *J. Chem. Phys.* **110** (1999) 6158 (http://dx.doi.org/10.1063/1.478522)
41. D. Marx, J. Hutter, Ab initio *molecular dynamics: basic theory and advanced methods*, Cambridge University Press, Cambridge, 2009 (http://dx.doi.org/10.1017/CBO9780511609633)
42. P. Carloni, U. Rothlisberger, M. Parrinello, *Acc. Chem. Res.* **35** (2002) 455 (http://dx.doi.org/10.1021/ar010018u)
43. F. Neese, *Wiley Interdiscipl. Rev. Comput. Mol. Sci.* **12** (2022) e1606 (http://dx.doi.org/10.1002/wcms.1606)
44. S. Kumar, *J. Serb. Chem. Soc.* **88** (2022) 381 (http://dx.doi.org/10.2298/JSC220921087K)
45. A. E. Reed, L. A. Curtiss, F. Weinhold, *Chem. Rev. (Washington, DC, U. S.)* **88** (1988) 899 (http://dx.doi.org/10.1021/cr00088a005)
46. S. Kumar Panja, S. Kumar, A. D. Fazal, S. Bera, *J. Photochem. Photobiol., A* **445** (2023) 115084 (http://dx.doi.org/10.1016/j.jphotochem.2023.115084)
47. P. L. A. Popelier, F. Aicken, S. O'Brien, *Atoms in molecules*, Vol. 188, Prentice Hall Manchester, 2000.